communications earth & environment

Article

https://doi.org/10.1038/s43247-024-01376-w

3.7 billion year old detrital sediments in Greenland are consistent with active plate tectonics in the Eoarchean

Check for updates

Austin Jarl Boyd [1] ✉, Minik T. Rosing [1], Magnus A. R. Harding [1,2], Donald E. Canfield[3] & Tue Hassenkam[1]

Plate tectonic processes modulate element cycling, crust generation, and differentiation, yet at what point in Earth's history these processes emerged remains debated. Here we present evidence that parts of the >3.7 Ga Isua Supracrustal Belt formed within a fore-arc setting, consistent with the operation of plate tectonics in the Eoarchean. We show that the oldest known sequence of detrital meta-sedimentary rocks were deposited conformably above chemical sediments on a volcanic basement. Mineral and trace elemental compositions show that turbiditic and pelagic detrital sediments were derived from terrains, comprising both basalts and differentiated tonalitic igneous rocks. The boninitic volcanic basement would have formed in a tensile environment before the adjacent terrains which sourced the clastic sediments. This suggests formation within a fore-arc during the initial few million years of subduction. This environment may have facilitated the local proliferation of life suggested by the frequent occurrence of layers rich in biogenic graphite.

On modern Earth, the crust moves laterally through the process of plate tectonics, in which oceanic crust is formed at spreading ridges and recycled in subduction zones. As a consequence of this recycling, volcanic island arcs, typically consisting of thickened and, on average, more differentiated igneous rocks form above subduction zones and may become further thickened and differentiated through accretion or collisions of other thickened crustal terrains[1,2]. These processes modulate climate[3] and the abundance of organic life, as the enhanced topography leads to increased weathering and erosion, causing sediments to be deposited in adjacent basins and increasing the flux of biologically essential nutrients to the ocean[4]. However, there is considerable disagreement on when plate tectonics started, with estimates ranging from 850 Ma to 4.2 Ga[5]. With a late origin of plate tectonics, many of the oldest preserved terrains are argued to have formed on a stagnant (i.e., immobile) crust, localized above long-lived zones of vertically upwelling mantle[6–10]. One of the oldest of such terrains is the 3.8 Ga to 3.7 Ga Isua Supracrustal Belt (ISB), which is a supracrustal enclave within the 3.9 Ga to 3.5 Ga Itsaq Gneiss Complex in Western Greenland (see maps in Fig. S1). While some have proposed that the ISB was formed through plate tectonic processes, above a subducting plate[11–16], others have recently suggested that the ISB formed through volcanism related to non-plate tectonic processes[17–19].

The ISB consists of tectonic panels mainly comprising mafic, ultramafic and felsic magmatic rocks, as well as subordinate chemical sediments[20]. Mafic and ultramafic lithologies form two chemically and geographically distinct suites; a tholeiitic suite with flat to slightly enriched rare earth element (REE) patterns and a boninite-like suite with u-shaped REE patterns[11,12,21,22]. Rock suites in the out-facing panel of the arcuate belt formed at ca. 3.81 Ga, whereas suites along the middle and inward-facing panels within the belt may have formed between 3.72 and 3.69 Ga[23]. Two regional metamorphic events have placed the entirety of the ISB within amphibolite facies at 3.7–3.6 Ga[24–26] and 2.8–2.6 Ga[27]. High tectonic strain, related to the metamorphic events, obscures original structures in many areas, making it difficult to discern the original protoliths, but augens of lesser strain, where sedimentary and igneous structures and textures are preserved, can be observed in many areas[28].

Detrital meta-sedimentary rocks, consisting of turbiditic and pelagic pelites, occur within sporadic outcrops in the western arm, along the middle of the belt. The pelites represent the oldest detrital sedimentary section discovered on Earth and have previously garnered attention because they host evidence of >3700 Ma life in the form of abundant ^{13}C-depleted graphite[29–31] and early evidence for biologically fixated nitrogen[31,32]. This graphite is particularly abundant within the pelagic pelites where it often occurs as laminar layers, interbedded with muscovite, chlorite and quartz.

[1]Globe Institute, University of Copenhagen, Copenhagen, Denmark. [2]Sino-Danish College (SDC), University of Chinese Academy of Sciences, Beijing, China. [3]Department of Biology, Nordic Center for Earth Evolution, University of Southern Denmark, Odense, Denmark. ✉e-mail: austin.boyd@sund.ku.dk

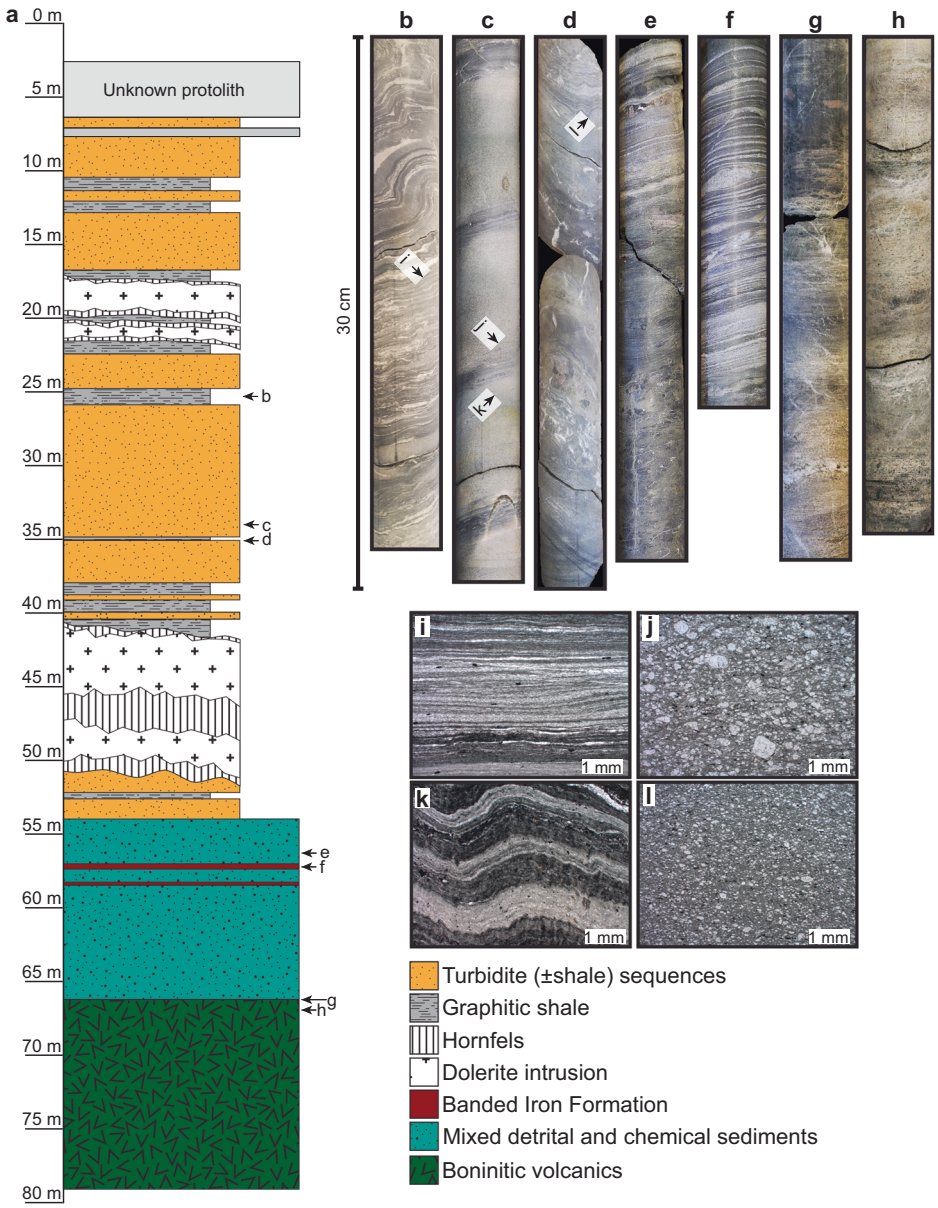

Fig. 1 | Examples of core lithologies and their distribution. a log of lithologies present in the rock core (see Supplementary note 1 for description of lithologies). **b**–**f** examples of lithologies displaying clear sedimentary structures. Locations indicated by arrows. **b** graphitic shales with quartz and calcite veins formed pre-deformation. **c** repeating turbiditic layers consisting of graded beds, topped by laminar beds. **d** chlorite-rich graphitic shales in bottom and muscovite-rich graphitic shales in top. Sedimentary texture in middle of lower block obliterated by metamorphic growth of green amphibole and garnet, likely stable because of high iron concentration. **e** Mixed detrital and chemical sediments in lower 10 cm consisting of green amphibole and chlorite. Interbedding with fine quartz (chert) layers in upper section suggests that amphibolite layers were deposited as volcaniclastics or detritals mixed with iron rich precipitates. **f** banded layers of magnetite and quartz, i.e., "banded iron formation". **g** transition between altered volcaniclastics in the bottom and mixed detrital and chemical sediments, in the form of green amphibolites, above. **h** gradual transition from boninitic volcanics in the bottom third to altered volcaniclastics above. **i** quartz, muscovite and graphite content varying on millimeter and sub-millimeter scales within graphitic shales. **j** basal section of graded bed consisting of plagioclase grains in matrix of chlorite and quartz. **k** coherent and finely bedded layers consisting of quartz, muscovite and graphite in graphitic shales. **l** top section of graded bed consisting of plagioclase grains in chlorite-quartz matrix. Note difference in grain size between **j** and **l**.

The deposition of turbiditic and pelagic pelites implies that the ISB, or parts of it, formed a basin which was proximal to thickened terranes from which detrital sediments were derived.

The detrital meta-sediments occur within a section of the ISB dominated by basaltic amphibolites with major and trace elemental compositions that are equivalent to those of boninites[11,12]. Boninites are volcanic rocks, primarily formed in fore-arcs through flux melting of mantle already depleted by partial melting and extraction of basaltic melts, during the first few million years after (re-)initiation of subduction[33]. Their presence within the ISB has therefore been used to argue for formation within a supra-subduction zone environment[11,12].

To determine whether the ISB formed in a supra-subduction zone setting, we examine the relation between detrital meta-sediments and adjacent volcanic boninites. Additionally, we determine the provenance of the detrital meta-sediments through major and trace elemental compositions. To that end we have obtained and analyzed two rock cores that transect the boundary between boninitic amphibolites and meta-sedimentary rocks on the western side of the belt. The two cores are perpendicular to each other, one at a low angle to the layering and one that is perpendicular to the layering, and separated by ca 200 m along the strike of the lithologic layering. We have focused our analysis on the core that was drilled perpendicular to the layering as transitions between lithologies are easier to observe (see Fig. 1). Two thirds of the length of this core consist of detrital meta-sediments, which we have sampled for major and trace elemental analysis.

Results and discussion

Conformable deposition from volcanic basement to detrital sedimentation

In Fig. 1 we present a lithological overview of the core. As in the rest of the ISB, all lithologies within the core have experienced strain, which is mostly expressed as shortening sub-perpendicular to the original layering. This original layering is, however, still clearly distinguishable, allowing us to observe and describe continuous and abrupt changes in mineral composition, structures and textures. The lower third of the core consists of green amphibolites with textures and structures that are equivalent to those of the meta-volcanic boninitic amphibolites that occur in outcrops surrounding the meta-sedimentary outcrop and can be considered part of the same suite of rocks. In the core, these amphibolites grade upwards into banded quartz – magnetite rocks (Fig. 1f), interpreted as chemical sediments (banded iron

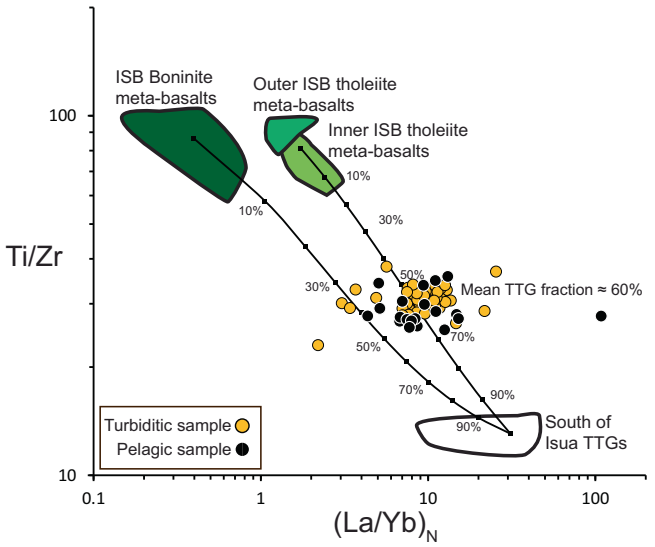

Fig. 2 | $(La/Yb)_N$ and Ti/Zr compositions of detrital meta-sedimentary samples compared to common rock compositions within and around the ISB. The right notched line shows simple mixing between average tholeiitic meta-basalts from the ISB and average TTGs sampled south of the ISB, whereas the left line models mixing between average ISB boninitic meta-basalt and TTGs. Percentages denote mass fraction of material derived from TTGs. The mean composition of detrital meta-sediments corresponds to a TTG mass fraction of ca. 60%. N in $(La/Yb)_N$ indicates normalization to primitive mantle[39]. Compositional fields for meta-basalts[11,12] and TTGs[40] correspond to samples distinguished as least altered by the authors. End-member data and calculation of mixing lines are included in Supplementary Data 2.

formation; BIF) which are interlayered with layered iron-rich green amphibolites derived from volcaniclastic material or mixed detrital-chemical sediments (Fig. 1e). The transition between boninitic amphibolites and the sediments above consists of ca. 2 m of interchanging finer grained layers of boninitic amphibolite, carbonate or quartz rich layers, and green amphibolites (equivalent to the mixed detrital-chemical lithology), with each layer making up 1 to 10 cm (Fig. 1g, h). These lithologies likely comprise volcaniclastics that were variably affected by seafloor weathering and alteration (e.g., ref. 34), and mixed with chemical sediments. Similar layers occur sporadically, and in thinner layers, for a few meters above this transition. We do not observe any variations in strain across the boundary, which is consistent with a conformable transition from volcanic to sedimentary deposition. The upper two thirds of the core are dominated by meta-sedimentary rocks with detrital protoliths consisting of turbiditic and pelagic mudstones (Fig. 1b, c). Turbidites in the middle third of the core consist of plagioclase-chlorite schists whereas turbidites in the upper core consist of clinozoisite-mica schists (see supplementary note 1 for detailed description). The turbiditic lithologies are often characterized by graded bedding (Fig. 1j, l), which provides clear evidence of a stratigraphic up (i.e., younging direction). The pelagic mudstones are graphite bearing muscovite-quartz schists and chlorite-quartz schists (Fig. 1b, d, i, k), which were deposited during quiescent intervals between turbiditic events. The undisturbed sedimentary bedding suggests all deposition took place below storm wave base (>100 m).

Our observations show that the volcanic protoliths of the boninitic amphibolites constitute the basement of the basin in which the sedimentary lithologies were deposited. A gradual decrease in the thickness and frequency of volcaniclastic layers and increase in the thickness and frequency of iron rich green amphibolite layers, interlayered with magnetite and quartz layers (BIFs; Fig. 1e, f), records a waning of local volcanic activity and a shift towards dominance of chemical sedimentation with detrital input. This depositional environment transitions gradually upwards into one dominated by detrital sedimentation, but layers affected by chemical precipitation and sedimentation of iron-rich minerals occur sporadically further up in the core, as can be inferred from occasional layers with comparatively high FeO concentrations relative to MgO or TiO_2 (Fig. S3).

Continuous deposition of iron-rich chemical precipitates concurrent with waning volcanism followed by the waning of chemical sedimentation, to be replaced by detrital deposition constitutes a gradual and conformable transition from the formation of the volcanic basement to the deposition of detrital sediments. This conformable transition is consistent with previous age determinations of the detrital meta-sediments and surrounding volcanic rocks, which have not resolved any difference in age between the two[29], but still allows for a considerable span in ages, due to the large uncertainty in whole rock isochron ages ($^{147}Sm/^{144}Nd$ age = 3779 ± 81 Ma, MSWD = 8.76; see also supplementary note 2). Given the age constraints and gradual transition in depositional character, we interpret the sedimentary sequence as having been deposited in a young volcanic basin where waning volcanic activity gradually allowed detrital sources to dominate the deposition. Given that detrital sedimentation initiated virtually immediately after volcanic cessation, the source of detrital sediments would have to have existed before or formed concurrent with formation of the volcanic basin. The shift in turbiditic composition from the middle to upper core could indicate a transition from sand to mud dominated deposits, which would indicate a deepening of the basin with time. This would be consistent with thermal relaxation of the newly formed crust either caused by migration of the active volcanic axis away from the site of deposition, or cessation of the boninitic volcanism altogether.

Mineral and trace elemental composition of detrital sediments

To constrain the depositional setting of the ISB detrital sediments, we investigated whether they were derived from volcanic rocks that are part of the same magmatic system as the volcanic basement on which they were deposited or from a separate terrain. For this purpose, we analyzed turbiditic layers (see "Supplementary Data 1" for major and trace elemental data) as they are derived from accumulated sediments at a higher topographic level and therefore most directly would sample the composition of adjacent terranes. In the rock core, the most well-preserved turbiditic layers are observed in the middle of the core, where they consist of plagioclase-chlorite schists (Fig. 1c, j and i). These contain abundant plagioclase clasts with sodic compositions (i.e., albite-oligoclase) and no observed K-feldspar. This is reflected by Na_2O concentrations up to 6 wt.%, and low average CaO (1.5 ± 1.0 (1σ) wt.%) and K_2O (1.1 ± 1.2 (1σ) wt.%) concentrations for whole rock samples. The abundance and composition of detrital plagioclase clasts and the absence of K-feldspar is consistent with a sedimentary source that contained felsic igneous rocks belonging to the tonalite-trondhjemite-granodiorite (TTG) suite[35]. The presence of this suite of differentiated igneous rocks in the sedimentary source terrain is also supported by trace elemental compositions. In particular Ti/Zr and REE patterns of the detrital metasediments are useful proxies for the relative contributions of mafic or felsic rock to their sources as their variation largely reflects igneous differentiation of the source rock and are minimally affected by hydrodynamic sorting[36,37]. In addition, these elements exhibit low mobility during metamorphic fluid flow and are therefore not susceptible to post-depositional modification[38]. In Fig. 2 we plot the Ti/Zr and La_N/Yb_N (representing REE patterns, N denotes normalization to primitive mantle[39]) composition of both turbiditic and pelagic samples and compare them to the compositions of 3.82 Ga TTGs sampled south of the ISB[40], ca. 3.81 Ga tholeiitic amphibolite from the ISB[11], ca. 3.7 Ga boninitic amphibolites from the ISB[12], and ca. 3.7 Ga tholeiitic amphibolites from the inner ISB panel[11]. The TTG compositions correspond to samples that display igneous textures (i.e., non-gneissic) and are therefore a good representation of TTGs that have not experienced any compositional alteration. Similarly, tholeiitic and boninitic compositions are those deemed least altered by their publishers and represent the breadth of mafic compositions found within the ISB. Our turbiditic samples cluster together at compositions that are intermediate between mafic and TTG compositions (Fig. 2). Pelagic samples, which were formed through slow accumulation of clays and other fine mineral grains,

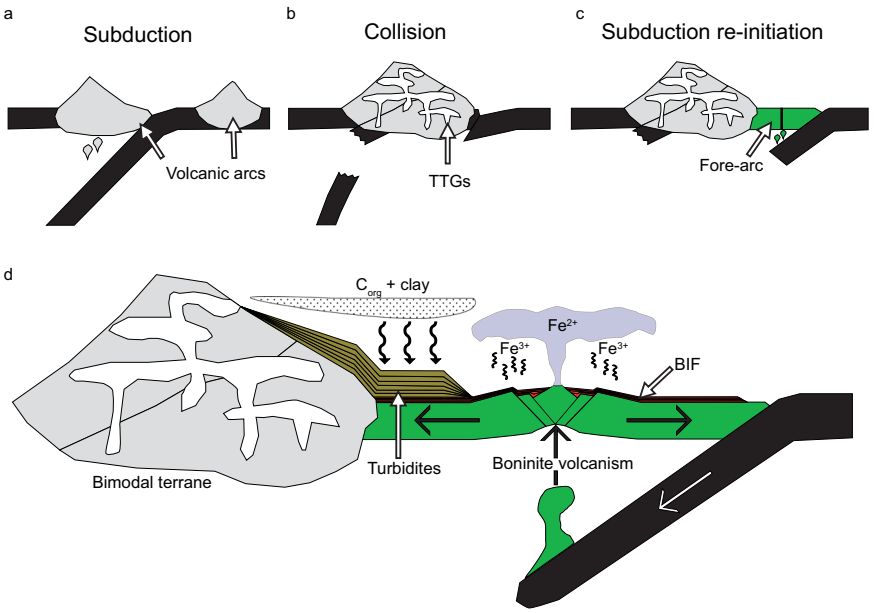

Fig. 3 | Schematic model of tectonic environment and timeline for formation of the ISB meta-sediments. a–c a possible sequence of events leading to the development of a fore-arc basin. **a** subduction transports volcanic arcs towards each other. One or both of these terranes could also have contained TTGs, given that TTGs within the Itsaq Gneiss Complex have ages up to 3.9 Ga[45]. **b** volcanic arcs collide, causing burial and melting of arc-derived basaltic rocks with compositions equivalent to the ISB tholeiitic suites, leading to the formation of TTGs. These TTGs could correspond to those within the Itsaq Gneiss Complex with ages 3.72 to 3.69 Ga[45]. **c** subduction is re-initiated on one side of the newly formed terrane, causing the formation of a fore-arc basin. **d** a diverging boninitic basement forms during the initial stages of subduction. Hydrothermal release of Fe causes enhanced precipitation of iron rich particles around the volcanic axis. As the basement moves further from the volcanic axis, sedimentation becomes dominated by turbidites that were ultimately derived from the nearby composite terrane. Pelagic clay and organic matter is deposited between turbiditic sequences.

plot within the same range of compositions, consistent with them receiving detrital material from the same terrain and with hydrodynamic particle sorting having minimal effect on the proxies used. Several of the turbiditic samples with lower La_N/Yb_N compositions have high iron concentrations, which suggests that a chemical sedimentary component could explain these lower compositions. The remaining samples are best modeled as a mixture of ca. 60% TTGs and ca. 40% mafic material with La/Yb ratios similar to the ISB tholeiitic amphibolites (Fig. 2). Conversely, mixing with material similar to the ISB boninitic amphibolite cannot explain the compositions measured for our samples (Fig. 2). The intermediate composition would be consistent with the presence of intermediately differentiated rocks in the sedimentary source area, but in that case plagioclase compositions would likely have been more calcic. The intermediate La_N/Yb_N and Ti/Zr compositions combined with the sodic plagioclase composition and abundance is thus consistent with a source terrain consisting of two compositional endmembers (bimodal), one differentiated, i.e., TTGs, and one primitive, i.e., mafic tholeiites with compositions similar to those within the ISB.

A differentiated bimodal terrain as source of detrital sediments

Formation of TTG melts requires water-saturated partial melting of tholeiitic basaltic rocks[41] or possibly fractional crystallization of hydrous arc tholeiite melts[42]. Indeed, modeling shows that the Archean TTGs surrounding the ISB, within the Itsaq Gneiss Complex, likely formed from melting of basaltic rocks with composition similar to those of the ISB tholeiitic suite[40,43] and could not have formed from partial melting of the ISB boninitic suite[40]. This is consistent with our result showing that the source terrain would have consisted of TTGs and tholeiitic basalts, and not boninitic basalts. In addition, the formation of TTGs requires differentiation of a mafic source at pressures above 1 GPa[43], suggesting crustal thickening of the sedimentary source terrain to more than 30 km, requiring sustained tectonism and/or magmatic activity. Previous work has shown that the detrital meta-sediments have $\varepsilon^{143}Nd$ values of ca. +1.6 to +2.1 and $\varepsilon^{176}Hf$ of −0.7 to +1.5[21], suggesting a fairly juvenile source, i.e., the source terrain was probably formed within the previous 200 Ma, consistent with the spectrum of zircon ages found within the ISB[23,44] and the TTGs within the surrounding Itsaq Gneiss Complex[16,45,46]. Indeed, the TTGs and ISB tholeiites display a similar range of $\varepsilon^{143}Nd$ and $\varepsilon^{176}Hf$ values, whereas the ISB boninites do not[15,21,47], which, again, is consistent with our data showing no boninitic material within the detrital meta-sediments.

The opening of a fore-arc basin

Multiple lines of evidence have previously been used to argue that the ISB, and the surrounding TTGs, were formed within a subduction zone setting. Major and trace elemental compositions of magmatic rocks are similar to those found in modern supra-subduction zones, which requires fluid fluxing of the mantle[11,12,14], rocks formed within differing environments and at different times were tectonically juxtaposed in the Eoarchean, requiring horizontal plate movement[16,23] and more recently there has been found evidence that atmospherically cycled sulfur was recycled into the Eoarchean mantle[48,49]. The supra-subduction zone model was challenged by the model of ref. 17, who suggested that the ISB could have formed by cycling through stages of rapid volcanic extrusion, above a mantle upwelling, followed by sinking of said volcanic rocks, leading to their partial melting, thus forming TTG melts. Such a model is, however, incompatible with the depositional sequence we have presented here. We have shown here that the detrital sediments were derived from a terrain that was unrelated to the volcanic basement and started to accumulate quickly after formation of the basement. If the sediments had been deposited within the model described by ref. 17 we would expect them to be derived from the volcanics that formed the basement as that volcanism either would be ongoing and producing nearby edifices, or entering dormancy after having built up nearby volcanic platforms.

Instead our observations show that the formation of the boninitic volcanic basement constituted the opening of a basin adjacent to a thickened terrain consisting of TTGs and the mafic tholeiites from which the TTGs were derived (see schematic model in Fig. 3). For the volcanic basement to have constituted a sedimentary basin, it must have formed within a tensional tectonic environment that did not allow build-up of volcanic products, which would dominate the detrital sediments. This is consistent with the gradual upwards decline in chemical Fe-sedimentation observed in the core, and is also corroborated by the observation of sheeted dyke complexes within the tholeiitic suite of the inner panels[13]. Further, the quick commencement of detrital deposition shows that the sedimentary source terrain was formed before the boninitic volcanic basement. We suggest that the sediments were deposited within a volcanic tensional environment similar to where modern boninites are formed, i.e., a fore-arc environment. Fore-arcs form between the main arc and trench in a supra-subduction zone during the first few million years after initiation of subduction[33], but it is unclear what causes such initiation. One suggestion is that subduction may

halt and then be re-initiated during collision of buoyant crustal blocks such as volcanic arcs or oceanic plateaus[50,51] (Fig. 3a, b, c). In this scenario, a new subduction zone could form on either side of the newly formed composite terrane. Such an event can also explain the occurrence of TTGs in the sedimentary source terrain as it has been suggested that these could form from burial and melting of enriched tholeiitic basalts during tectonic thickening[40], as described above. TTGs in the gneiss complex that surrounds the ISB today have formed in intervals every 40–50 Ma, but over a protracted period of ca. 200 Ma[16,45,46], which would suggest that collisional events occurred regularly in the Eoarchean geodynamic environment. This would then also explain how the ISB itself came to be preserved within the crust as its position in a fore-arc between a main arc and a trench would allow it to become sandwiched between terrains during their collision and accreted onto older gneissic TTG continental nuclei. Similarly, Phanerozoic ophiolites mostly consist of fore-arc crust, which have been preserved during the collision of two terrains[50]. In this model the 3.7 Ga section of the ISB could have experienced a lower grade of metamorphism during its tectonic emplacement than the 3.81 Ga section, which is consistent with recent work suggesting that the younger section did not experience peak metamorphism before 2.6 Ga[52]. The geodynamic sequence of collision, fore-arc extension and subduction recorded within the Itsaq Gneiss Complex and ISB is thus strikingly similar to the sequence produced by modern convergent plate tectonic environments. As such, the successions sampled by our drill core provides the oldest known sedimentary record of plate tectonic processes taking place on Earth.

Implications for earliest known biosphere

It is unclear whether it was possible for land to become exposed above sea level in the early Archean[53], but it has recently been suggested that substantial sub-aerial weathering of differentiated crust was active since at least 3.7 Ga[54]. The existence of the sedimentary succession described here may substantiate this claim as the formation of detrital sediments, through the processes of erosion and transport, mostly takes place during exposure of rocks above the surface of the ocean. However, the existence of detrital sediments on its own is only circumstantial evidence of such exposure. If the ISB detrital sediments indeed were formed from sub-aerial exposure of the source terrain, it could possibly have provided an enhanced flux of nutrients to the adjacent waters, which may have fueled the pelagic life-forms from which organic matter continuously accumulated within the ISB sediments between turbiditic events. In any case, it is possible that the active tectonism and magmatism provided a nutrient rich basin that allowed for the local proliferation of life.

Methods

Sample acquisition

Our sample material is derived from a rock core that was drilled at a right angle to the layering. Rock was recovered from 2.68 m to 79.07 m below the surface. The core was logged on a cm scale and representative samples for major and trace elemental analysis were taken from each of the major logged lithologies, with care taken to acquire homogenous samples with no post-deformational veins. Single layer samples were preferred, but in the case of graphite schists, this was not possible as layering occurred on a submillimeter scale.

Major and trace elemental analysis

Digestions were performed in batches consisting of 13 rock powder samples, nine of which were digested in two aliquots, two that were digested in three aliquots and two that were digested in four aliquots. For each batch, four "blank" vessels and two aliquots of each of the two rock standards USGS Brush Creek Shale (SBC-1) and USGS Boquillas shale (ShBOQ-1) were subjected to the same treatment. 100 mg of sample powder was added to Teflon vessels with 1.5 mL conc. HNO_3, 0.5 mL HCl and 1.0 mL HF. Vessels were placed in a carousel within a Mars 6 microwave digestion system, which increased the temperature to 200 °C over 25 min and held the temperature for 30 additional minutes. 10 mL 4% boric acid was then added to all vessels. One aliquot from each of the samples that were digested in four aliquots was spiked with 100 µL of three different ISO certified standard solutions HA containing 1000 mg L^{-1} Al, Ca, Fe, K, Mg, Na and P and 100 mg L^{-1} As, B, Ba, Be, Bi, Cd, Ce, Co, Cr, Cs, Cu, Dy, Er, Eu, Ga, Gd, Ho, La, Li, Lu, Mn, Nd, Ni, Pb, Pr, Rb, Re, Se, Sm, Sr, Tb, Th, Tl, Tm, U, V, Y, Yb and Zn; HB containing 1000 mg L^{-1} Si and Ti and 100 mg L^{-1} Ag, Ge, Hf, Mo, Nb, Sn, Ta, Te, W, Zr; HC containing 100 mg L^{-1} Au, Os, Pd, Pt and Ru. Another aliquot of the same samples was spiked with 1000 µL of the same solutions. Vessels were then added back into the microwave carrousel, heated to 170 °C over 15 min, and held at that temperature at an additional 30 min. 0.5 mL aliquots from each vessel were diluted by x20 and x200 with milli-Q water and analyzed with an Agilent 7900 ICP-MS. Sample measurement output was calibrated to multi elemental standard solutions prepared from standards HA, HB, and HC and diluted to various compositions bracketing the expected range of diluted sample concentrations. Internal standardization was achieved through on-line introduction of Sc to the sample flow.

Data availability

Major and trace elemental concentration data related to this publication is published alongside it as supplementary files and can also be attained from the repository address https://doi.org/10.17894/ucph.bbe284ae-c91b-41bb-8e78-8fedf6824e48.

Received: 31 October 2023; Accepted: 8 April 2024;
Published online: 15 April 2024

References

1. Moyen, J.-F. et al. Collision vs. subduction-related magmatism: two contrasting ways of granite formation and implications for crustal growth. *Lithos* **277**, 154–177 (2017).
2. Kusky, T. & Wang, L. Growth of continental crust in intra-oceanic and continental-margin arc systems: analogs for archean systems. *Sci. China Earth Sci.* **65**, 1615–1645 (2022).
3. Macdonald, F. A., Swanson-Hysell, N. L., Park, Y., Lisiecki, L. & Jagoutz, O. Arc-continent collisions in the tropics set Earth's climate state. *Science* **364**, 181–184 (2019).
4. Hartmann, J., Moosdorf, N., Lauerwald, R., Hinderer, M. & West, A. J. Global chemical weathering and associated P-release — The role of lithology, temperature and soil properties. *Chem. Geol.* **363**, 145–163 (2014).
5. Palin, R. M. et al. Secular change and the onset of plate tectonics on Earth. *Earth-Sci. Rev.* **207**, 103172 (2020).
6. Bédard, J. H. Stagnant lids and mantle overturns: implications for Archaean tectonics, magmagenesis, crustal growth, mantle evolution, and the start of plate tectonics. *Geosci. Front.* **9**, 19–49 (2018).
7. Moore, W. B. & Webb, A. A. G. Heat-pipe Earth. *Nature* **501**, 501–505 (2013).
8. Wiemer, D., Schrank, C. E., Murphy, D. T., Wenham, L. & Allen, C. M. Earth's oldest stable crust in the Pilbara Craton formed by cyclic gravitational overturns. *Nat. Geosci.* **11**, 357–361 (2018).
9. Tarduno, J. A. et al. Hadaean to Palaeoarchaean stagnant-lid tectonics revealed by zircon magnetism. *Nature* **618**, 531–536 (2023).
10. Bédard, J. H. A catalytic delamination-driven model for coupled genesis of Archaean crust and sub-continental lithospheric mantle. *Geochim. et Cosmochim. Acta* **70**, 1188–1214 (2006).
11. Polat, A. & Hofmann, A. W. Alteration and geochemical patterns in the 3.7–3.8 Ga Isua greenstone belt, West Greenland. *Precambrian Res.* **126**, 197–218 (2003).
12. Polat, A., Hofmann, A. W. & Rosing, M. T. Boninite-like volcanic rocks in the 3.7–3.8 Ga Isua greenstone belt, West Greenland: geochemical evidence for intra-oceanic subduction zone processes in the early Earth. *Chem. Geol.* **184**, 231–254 (2002).

13. Furnes, H., de Wit, M., Staudigel, H., Rosing, M. & Muehlenbachs, K. A vestige of Earth's Oldest Ophiolite. *Science* **315**, 1704–1707 (2007).
14. Furnes, H., Rosing, M., Dilek, Y. & de Wit, M. Isua supracrustal belt (Greenland)—A vestige of a 3.8 Ga suprasubduction zone ophiolite, and the implications for Archean geology. *Lithos* **113**, 115–132 (2009).
15. Hoffmann, J. E., Münker, C., Polat, A., Rosing, M. T. & Schulz, T. The origin of decoupled Hf–Nd isotope compositions in Eoarchean rocks from southern West Greenland. *Geochim. et Cosmochim. Acta* **75**, 6610–6628 (2011).
16. Nutman, A. P. et al. Fifty years of the Eoarchean and the case for evolving uniformitarianism. *Precambrian Res.* **367**, 106442 (2021).
17. Webb, A. A. G., Müller, T., Zuo, J., Haproff, P. J. & Ramírez-Salazar, A. A non–plate tectonic model for the Eoarchean Isua supracrustal belt. *Lithosphere* **12**, 166–179 (2020).
18. Zuo, J. et al. Tectonics of the Isua Supracrustal Belt 2: microstructures reveal distributed strain in the absence of major fault structures. *Tectonics* **40**, e2020TC006514 (2021).
19. Ramírez-Salazar, A. et al. Tectonics of the Isua Supracrustal Belt 1: P-T-X-d Constraints of a Poly-Metamorphic Terrane. *Tectonics* **40**, e2020TC006516 (2021).
20. Rosing, M. T., Rose, N. M., Bridgwater, D. & Thomsen, H. S. Earliest part of Earth's stratigraphic record: a reappraisal of the >3.7 Ga Isua (Greenland) supracrustal sequence. *Geology* **24**, 43–46 (1996).
21. Hoffmann, J. E. et al. Highly depleted Hadean mantle reservoirs in the sources of early Archean arc-like rocks, Isua supracrustal belt, southern West Greenland. *Geochim. et Cosmochim. Acta* **74**, 7236–7260 (2010).
22. Szilas, K., Kelemen, P. B. & Rosing, M. T. The petrogenesis of ultramafic rocks in the >3.7 Ga Isua supracrustal belt, southern West Greenland: geochemical evidence for two distinct magmatic cumulate trends. *Gondwana Res.* **28**, 565–580 (2015).
23. Nutman, A. P. & Friend, C. R. L. New 1:20,000 scale geological maps, synthesis and history of investigation of the Isua supracrustal belt and adjacent orthogneisses, southern West Greenland: a glimpse of Eoarchaean crust formation and orogeny. *Precambrian Res.* **172**, 189–211 (2009).
24. Frei, R., Bridgwater, D., Rosing, M. & Stecher, O. Controversial Pb-Pb and Sm-Nd isotope results in the early Archean Isua (West Greenland) oxide iron formation: preservation of primary signatures versus secondary disturbances. *Geochim. et Cosmochim. Acta* **63**, 473–488 (1999).
25. Frei, R. & Rosing, M. T. The least radiogenic terrestrial leads; implications for the early Archean crustal evolution and hydrothermal–metasomatic processes in the Isua Supracrustal Belt West Greenland. *Chem. Geol.* **181**, 47–66 (2001).
26. Crowley, J. L., Myers, J. S. & Dunning, G. R. Timing and nature of multiple 3700–3600 Ma tectonic events in intrusive rocks north of the Isua greenstone belt, southern West Greenland. *Geol. Soc. Am. Bull.* **114**, 1311–1325 (2002).
27. Frei, R., Rosing, M. T., Waight, T. E. & Ulfbeck, D. G. Hydrothermal-metasomatic and tectono-metamorphic processes in the Isua supracrustal belt (West Greenland): a multi-isotopic investigation of their effects on the earth's oldest oceanic crustal sequence. *Geochim. et Cosmochim. Acta* **66**, 467–486 (2002).
28. Myers, J. S. Protoliths of the 3.8–3.7 Ga Isua greenstone belt, West Greenland. *Precambrian Res.* **105**, 129–141 (2001).
29. Rosing, M. T. 13C-Depleted Carbon Microparticles in >3700-Ma sea-floor sedimentary rocks from West Greenland. *Science* **283**, 674–676 (1999).
30. Ohtomo, Y., Kakegawa, T., Ishida, A., Nagase, T. & Rosing, M. T. Evidence for biogenic graphite in early Archaean Isua metasedimentary rocks. *Nat. Geosci.* **7**, 25–28 (2014).
31. Hassenkam, T., Andersson, M. P., Dalby, K. N., Mackenzie, D. M. A. & Rosing, M. T. Elements of Eoarchean life trapped in mineral inclusions. *Nature* **548**, 78–81 (2017).
32. Stüeken, E. E., Boocock, T., Szilas, K., Mikhail, S. & Gardiner, N. J. Reconstructing nitrogen sources to earth's earliest biosphere at 3.7 Ga. *Front. Earth Sci.* **9**, 675726 (2021).
33. Reagan, M. K. et al. Forearc ages reveal extensive short-lived and rapid seafloor spreading following subduction initiation. *Earth Planet. Sci. Lett.* **506**, 520–529 (2019).
34. Alt, J. C. & Teagle, D. A. H. The uptake of carbon during alteration of ocean crust. *Geochim. et Cosmochim. Acta* **63**, 1527–1535 (1999).
35. Moyen, J.-F. Archean granitoids: classification, petrology, geochemistry and origin. *Geol. Soc. Lond. Special Publ.* **489**, 15–49 (2020).
36. McLennan, S. M. Relationships between the trace element composition of sedimentary rocks and upper continental crust. *Geochem. Geophys. Geosyst.* **2**, 2000GC000109 (2001).
37. Greber, N. D. & Dauphas, N. The chemistry of fine-grained terrigenous sediments reveals a chemically evolved Paleoarchean emerged crust. *Geochim. et Cosmochim. Acta* **255**, 247–264 (2019).
38. Polat, A., Hofmann, A. W., Münker, C., Regelous, M. & Appel, P. W. U. Contrasting geochemical patterns in the 3.7–3.8 Ga pillow basalt cores and rims, Isua greenstone belt, Southwest Greenland: implications for postmagmatic alteration processes. *Geochim. et Cosmochim. Acta* **67**, 441–457 (2003).
39. Palme, H. & O'Neill, H. S. C. Cosmochemical estimates of mantle composition. In *Treatise on Geochemistry* 1–39 (Elsevier, 2014). https://doi.org/10.1016/B978-0-08-095975-7.00201-1.
40. Hoffmann, J. E., Nagel, T. J., Münker, C., Næraa, T. & Rosing, M. T. Constraining the process of Eoarchean TTG formation in the Itsaq Gneiss Complex, southern West Greenland. *Earth Planet. Sci. Lett.* **388**, 374–386 (2014).
41. Moyen, J.-F. & Martin, H. Forty years of TTG research. *Lithos* **148**, 312–336 (2012).
42. Jagoutz, O. et al. TTG-type plutonic rocks formed in a modern arc batholith by hydrous fractionation in the lower arc crust. *Contrib. Mineral Petrol* **166**, 1099–1118 (2013).
43. Nagel, T. J., Hoffmann, J. E. & Münker, C. Generation of Eoarchean tonalite-trondhjemite-granodiorite series from thickened mafic arc crust. *Geology* **40**, 375–378 (2012).
44. Nutman, A. P., Friend, C. R. L. & Paxton, S. Detrital zircon sedimentary provenance ages for the Eoarchaean Isua supracrustal belt southern West Greenland: Juxtaposition of an imbricated ca. 3700Ma juvenile arc against an older complex with 3920–3760Ma components. *Precambrian Res.* **172**, 212–233 (2009).
45. Nutman, A. P., Friend, C. R. L., Kinny, P. D. & McGregor, V. R. Anatomy of an Early Archean gneiss complex: 3900 to 3600 Ma crustal evolution in southern West Greenland. *Geology* **21**, 415–418 (1993).
46. Nutman, A. P., McGregor, V. R., Friend, C. R. L., Bennett, V. C. & Kinny, P. D. The Itsaq Gneiss Complex of southern West Greenland; the world's most extensive record of early crustal evolution (3900-3600 Ma). *Precambrian Res.* **78**, 1–39 (1996).
47. Hoffmann, J. E. et al. Mechanisms of Archean crust formation inferred from high-precision HFSE systematics in TTGs. *Geochim. et Cosmochim. Acta* **75**, 4157–4178 (2011).
48. Lewis, J. A. et al. Sulfur isotope evidence for surface-derived sulfur in Eoarchean TTGs. *Earth Planet. Sci. Lett.* **576**, 117218 (2021).
49. Lewis, J. A. et al. Sulfur isotope evidence from peridotite enclaves in southern West Greenland for recycling of surface material into Eoarchean depleted mantle domains. *Chem. Geol.* **633**, 121568 (2023).
50. Stern, R. J. Subduction initiation: spontaneous and induced. *Earth Planet. Sci. Lett.* **226**, 275–292 (2004).
51. Stern, R. J. & Gerya, T. Subduction initiation in nature and models: a review. *Tectonophysics* **746**, 173–198 (2018).
52. Eskesen, B. et al. Neoarchean synkinematic metamorphic peak in the Isua supracrustal belt (West Greenland). *Geology* **51**, 1017–1021 (2023).
53. Korenaga, J. Was there land on the early earth? *Life* **11**, 1142 (2021).

54. Roerdink, D. L., Ronen, Y., Strauss, H. & Mason, P. R. D. Emergence of felsic crust and subaerial weathering recorded in Palaeoarchaean barite. *Nat. Geosci.* **15**, 227–232 (2022).

Acknowledgements
We thank Thor Frickmann for assistance with lab work, ICP-MS measurements and data reduction. This project was made possible through financial support provided by the Novo Nordisk foundation through NERD grant NNF21OC0068372. Research and export permits for rock core materials were granted by the Greenlandic self-government.

Author contributions
A.J.B. led the writing of the paper, with regular feedback from T.H., A.J.B., T.H. and M.T.R contributed to data interpretation, M.T.R. collected the sample material, M.A.R.H. and A.J.B. conducted sample preparation and characterization, D.E.C. provided analytical facilities. A.J.B. carried out sample digestion. All authors provided editing and review of the paper.

Competing interests
The authors declare no competing interests.

Additional information
Supplementary information The online version contains supplementary material available at https://doi.org/10.1038/s43247-024-01376-w.

Correspondence and requests for materials should be addressed to Austin Jarl Boyd.

Peer review information *Communications Earth & Environment* thanks the anonymous reviewers for their contribution to the peer review of this work. Primary Handling Editors: Joe Aslin, Carolina Ortiz Guerrero. A peer review file is available.